Received: 2 August 2022 | Revised: 3 October 2022 | Accepted: 10 October 2022

DOI: 10.1111/fwb.14013

ORIGINAL ARTICLE

Freshwater Biology WILEY

A two-dimensional morphospace for cyanobacteria and microalgae: Morphological diversity, evolutionary relatedness, and size constraints

Gábor Borics[1,2] | Gábor Várbíró[1] | János Falucskai[3] | Zsolt Végvári[1,4] | Enikő T-Krasznai[1] | Judit Görgényi[1] | Viktória B-Béres[1] | Verona Lerf[1]

[1]Centre for Ecological Research, Institute of Aquatic Ecology, Department of Tisza Research, Debrecen, Hungary

[2]University of Nyíregyháza, Nyíregyháza, Hungary

[3]Institute of Mathematics and Informatics, University of Nyíregyháza, Nyíregyháza, Hungary

[4]Senckenberg Deutsches Entomologisches Institut, Müncheberg, Germany

Correspondence
Gábor Várbíró, Centre for Ecological Research, Institute of Aquatic Ecology, Department of Tisza Research, 18/c Bem Square, H-4026 Debrecen, Hungary.
Email: varbirog@gmail.com

Abstract

1. Body metrics are considered as *master traits* that regulate physiological, behavioural and life history features of planktic cyanobacteria and microalgae. Although the distribution of their morphological traits reflects the various trade-offs and strategies needed for survival in pelagic habitats, previous methods for quantifying phytoplankton body shape do not adequately represent the intricate details of surface variation that are so important for their nutrient- and light-harvesting capabilities. Therefore, here we provide a new framework to quantify and illustrate the morphological diversity of cyanobacteria and microalgae.
2. Essential components of formulae used for surface area ($A = Cs \times d^2$) and volume ($V = Cv \times d^3$) calculations are provided by the shape-specific surface area and volume constants (*Cs*, *Cv*). *Cs*, the surface shape factor, characterises the *coarseness* of the object surface, and *Cv*, the volumetric shape factor, characterises the shape deviation from a sphere. Using these morphologically and biologically relevant variables, we defined a two-dimensional morphological space, in which all three-dimensional objects have well-defined positions.
3. By analysing morphologies of taxa representing various forms in major cyanobacterial and microalgal groups, we demonstrated that these groups show considerable differences in the area occupied within the morphospace and these differences are not affected by evolutionary relatedness. We showed that the ratio of surface and volume constants correlated with organism size, suggesting that the development of basic morphologies is constrained by their linear dimensions.
4. Using surface and volumetric shape factors, we created a two-dimensional Euclidean morphospace in which all three-dimensional objects have a specific position. Positioning uni- and multicellular cyanobacteria and microalgae of various shapes into this morphospace allows their geometrical and ecological limitations to be understood. Because of the close linkage between phytoplankton

morphology and ecology, the proposed morphospace may serve as a proxy for an ecospace. Thus, in future the proposed morphospace can be used to visualise current ecological processes such as eutrophication or seasonal succession of phytoplankton.

KEYWORDS
3D algae, geometry, morphological traits, phylogenetic control, shape complexity

1 | INTRODUCTION

Across the animal and plant kingdoms, the evolution of body shape in organisms is constrained by geometry. Although the relationships among shape complexity and geometry have been investigated in a number of taxa (avian egg shape: Stoddard et al., 2017; squamates: Watanabe et al., 2019), only a few attempts have been made to elucidate the interplay between evolution and geometry of microalgae (Naselli-Flores et al., 2021; Ryabov et al., 2021), which include perhaps the most geometrically diverse groups of organisms on Earth. Phytoplankton are one of the most ancient biotic assemblages of our planet. Its earliest representatives, cyanobacteria, developed oxygenic photosynthesis, which is considered to be the most important metabolic innovation that formed the Earth's oxygenic atmosphere, shaping the evolution of life. The endosymbiotic relationship between cyanobacteria and heterotrophic eukaryotes triggered microalgal evolution and resulted in various lineages (Falkowski et al., 2004). Planktic cyanobacteria and microalgae exhibit a wide variety of genetic, morphological or behavioural differences that enable them to inhabit almost every habitat type where water occurs in liquid form and light is available. During their 3 billion-year long evolution (Planavsky et al., 2014), oxygenic microscopic photosynthesisers developed a wide array of adaptations to survive severe conditions, such as extremely high temperature (Gerloff-Elias et al., 2006), salinity, extreme pH, nutrient deficiency (Mitsui et al., 1986; Padisák & Naselli-Flores, 2021; Raven, 2010), desiccation, as well as high or low levels of radiation (Hoek et al., 1995). Besides these specialised physiological traits, life history (resting stages, asexual/sexual reproduction) and behavioural traits (motility, mixotrophy) also allowed cyanobacteria and microalgae to cope with the constraints imposed by various aquatic habitats (Litchman & Klausmeier, 2008). In addition, planktic cyanobacteria and microalgae exhibit highly variable body metrics, such as size and shape, which are directly affected by the physical characteristics of their environments, such as hydrostatic pressure (Koch et al., 1982), gravitational acceleration, density and viscosity of water, and the size of the filtering apparatus of grazers (Reynolds, 2006). Body metrics are considered as *master traits* that regulate physiological, behavioural and life history features of planktic cyanobacteria and microalgae. The distribution of morphological traits in the phytoplankton reflects the various trade-offs and strategies needed for the phytoplankters to survive in pelagic habitats (Litchman et al., 2007). While individual biovolume is a reliable and broadly accepted measure of the size of organisms (diatoms: Rimet & Bouchez, 2012; planktic microalgae: Borics et al., 2021; coenobial cyanobacteria: T-Krasznai et al., 2022), morphological complexity lacks a straightforward definition. Approximation of the form of microalgae with appropriate geometric shapes is a frequently used approach (Hillebrand et al., 1999; Sun & Liu, 2003). Indeed, shape complexity can be examined and defined by applying perceptual, computational, or statistical approaches. To date, several shape attributes have been proposed to quantify the morphological complexity of three-dimensional (3D) objects, such as surface variation, symmetry, part count, simpler part decomposability, intricate details, and topology (Sukumar et al., 2008). Although several of these dimensions are visually plausible, surface variation and intricate details have utmost importance for the nutrient- and light-harvesting capabilities of photosynthetic phytoplankters, yet they are not well described by these previous methods of measurement.

Although the visual appearance of cyanobacteria and microalgae suggests huge morphological diversity, the numerical characterisation of this feature is still a challenging problem (Ryabov et al., 2021). Therefore, here we provide a framework to quantify and illustrate the morphological diversity of cyanobacteria and microalgae. By constructing 95 real-like 3D models of microalgae and cyanobacteria representing the most relevant 21 lineages, we can calculate their surface area- and volume-specific constants as two axes of a morphospace. Placing the representatives of the groups into this morphospace, the areas of the polygons defined by the species can be estimated and used as a proxy of morphological diversity. We discuss the relationships between morphological diversity and the phylogenetic position of the selected taxonomic groups. Finally, we discuss how the longest linear dimensions of the various morphologies that exist in natural planktonic assemblages limit their performance in the pelagic environment.

2 | MATERIALS AND METHODS

2.1 | Theory

Morphological complexity increases with organismal size both at macro- (Carroll, 2001) and microscales (Karp-Boss & Boss, 2016). Size of planktic organisms, however, is limited by various factors. The turbulence-related physical conditions in water are among the most important constrains (Naselli-Flores et al., 2021; Naselli-Flores & Barone, 2011). To avoid physical injuries, cells and colonies are predicted to be smaller than the smallest turbulent eddy, ranging between 0.2 and 0.4 mm (Reynolds, 1998a). The quadratic relationship between the size of particles and velocity of their sinking also controls organism size (Durante et al., 2019). The longest linear dimensions of planktic photosynthesisers therefore rarely exceed 400 µm. Maximum size can also be limited by metabolic rate, because the specific surface area decreases with increasing volume (Reynolds, 2006), which also increases the time of molecular transport within the cells (Gallet et al., 2017; Pasciak & Gavis, 1974). Besides their size, the shape of microalgae also influences their sinking velocity, production of mucilage, vacuoles, storage products, and other vital components (Reynolds, 2006).

In contrast to size, shape is not an easily measurable feature of the objects. Among the various quantifiable measures of shape complexity, surface variation plays a crucial role for cyanobacteria and microalgae. Increasing morphological complexity coincides with an increase in surface area/volume ratio, which is an advantageous evolutionary adaptation to light or nutrient deficient environments (Grover, 1989; Sournia, 1982) that might represent a competitive advantage for planktic organisms. Surface area and volume of any 3D objects are proportional to the second and third power of their linear dimensions (Equations (1) and (2)).

$$A = Cs \times d^2 \tag{1}$$

$$V = Cv \times d^3 \tag{2}$$

where

A: surface area of the object.

d: maximal linear dimension of the objects.

Cs: shape-specific surface area constant.

V: volume of the object.

Cv: shape-specific volume constant.

The above formula provides a perfect one-to-one relationship between linear dimension and volume of an object. Although the specific constants are not known for complex shapes, the equations: $Cv = V/d^3$; and $Cs = A/d^2$ allow the computation of the constants supposing that their volumes and surface areas are known or can be computed.

2.2 | Surface and volume calculations of cyanobacteria and microalgae

The volume and surface area of objects can be exactly computed by using real-like 3D images (Borics et al., 2021). We used Blender 2.90 software to create realistic 3D models of cyanobacteria and microalgae (Blender Foundation and Community, 2020). It is a free open-source 3D graphics application, which allows the generation of 3D *mesh* objects. Using graphical presentation and photographs in identification books and observation of species by microscopes, we constructed 95 algal 3D models of different shapes representing the major taxonomic groups. Using the NeuroMorph software toolset (Jorstad et al., 2015), we measured the surface area and volume of each object (Appendix S1).

2.3 | Morphological complexity in a two-dimensional morphospace

Morphology of all 3D objects can be characterised by the *Cs* and *Cv* dimensionless metrics. Using them as axes in an orthogonal coordinate system, a two-dimensional (2D) morphospace can be defined, in which 3D objects can be represented by a single point (Figure 1).

Supposing that any object is infinitely divisible, theory shows that the sum of the surface areas of their internal objects converge to infinity. Thus, while *Cv* of the objects has well defined maxima ($\Pi/6$), their surface constants (*Cs*) might converge to infinity, independently

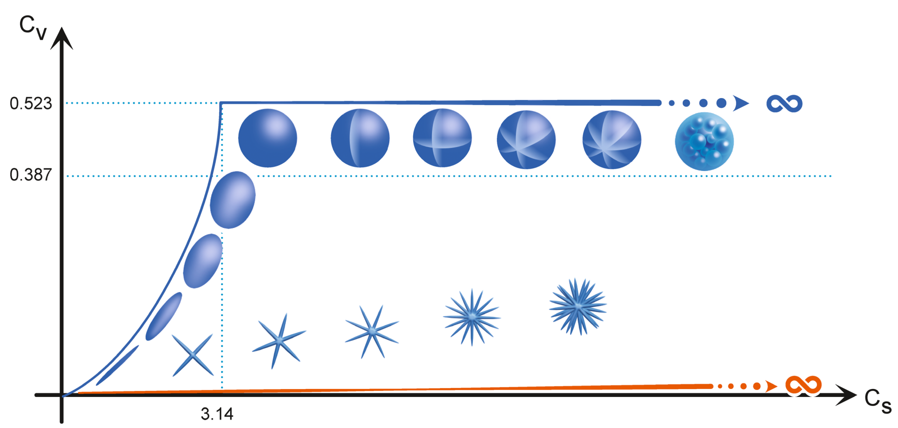

FIGURE 1 Two-dimensional morphospace of three-dimensional (3D) objects defined by their surface area (*Cs*) and volume constants (*Cv*). The sphere has a specific location in the morphospace ($Cs = \Pi$; $Cv = \Pi/6 = 0.523$) because it denotes the possible highest *Cv* value ($\Pi/6$) of 3D objects, supposing that d in the Equations (1) and (2) denotes the longest linear dimension of the object. The horizontal line at $Cv = 0.387$ indicates the *Cv* values of spherical colonies filled with densely packed spheres. Coordinates of prolate spheroids with decreasing ellipticity define the borderline of the geometrically possible shapes, as values of *Cs* and *Cv* of an infinitely long and infinitely thin prolate spheroid converge to zero. Among the infinite number of 3D objects with a specific value of *Cs*, prolate spheroids have the largest *Cv* values, therefore shapes cannot occur in the area left of the borderline defined by the $Cv = f(Cs)$ formula given for prolate spheroids (Figure S1)

of their Cv values. For example, coordinates of Menger sponge-like fractal bodies having an infinitely small volume Cv ($Cv \rightarrow 0$) and an infinitely large surface area ($Cs \rightarrow \infty$) are located along the Cs axis, infinitely close to it. According to Kepler's conjecture, the volume of the densest possible sphere packing is $\Pi/3/\sqrt{2} \approx 0.74$ (Kepler, 1611; Sloane, 1998); Cv values of densely packed spheres therefore cannot exceed the $\Pi/6 \times 0.74 = 0.387$ value. However, coordinates of living organisms are not arbitrarily scattered throughout this 2D space. Cells are the smallest units of living organisms. Their shapes and the way they proliferate and aggregate predicts the shape of living creatures and the borders of the region in the Cs/Cv space where they might potentially occur. In the world of microalgae, there is a continuous transition from the spindle-like forms (with extremely low Cs and Cv values) through prolate spheroids to a sphere (the exact mathematical description is provided in Figure S1). Spindle, sphere, and spherical cell aggregates constitute the three corners of the subregion where coordinates of real objects occur. However, as cellular functioning needs a minimum cell size, elongated filamentous forms should not be thinner than 0.5 μm and the diameter of the spherical cells in colonies should not be smaller than 0.7–1 μm. Since elongated filamentous forms have the smallest Cv and Cs values, the creation of star-like colonies by the addition of a new filament results in a linear increase in Cv values, defining the third theoretical side of the morphospace.

2.4 | Selection of cyanobacterial and microalgal forms

Mapping the morphological diversity of freshwater cyanobacteria and various microalgal groups in the proposed morphospace needs the enumeration of each morphological category occurring in the given phylogenetic groups. Using the most recent taxonomic handbooks, we selected one representative taxon for each morphologically different category from the group and created their real-like 3D models. Thus, we selected: (1) one sphere-like species, an elongated form that has the largest length/width ratio based on the literature; (2) a coenobial species having the largest cell numbers; and (3) star-like forms with the largest numbers of radii (names selected species and their 3D images are shown in Supplementary Material 1). However, we had to consider that although an increase in cell numbers increases the volume and surface area of the multicellular colonies, in the case of several groups the colonies might change organisation type from dense to vesiculate coenobia, which reduces their Cs and Cv values. Therefore, for example in the case of *Synura* colonies (Chrysophyceae) we calculated with 32 cell numbers, although larger colonies do exist.

After measuring their accurate volumes and surface areas, we calculated their Cv and Cs values and projected them onto the 2D morphospace. Afterwards, we created a minimum of three objects in each group, connecting their points, which allowed the delineation of polygons of various shapes and sizes. We calculated the area of the polygons as representations of the morphological diversity of the groups. Calculations were done using the R statistical programming environment (R Core Team, 2018). To investigate the morphological/taxonomical diversity relationship, we applied the groups' species numbers given in the latest updated version of Algaebase (Guiry & Guiry, 2008).

2.5 | Phylogenetic relatedness of the morphologies

To evaluate how phylogenetic relatedness is associated with morphological diversity of cyanobacteria and microalgae, we first constructed a phylogenetic tree combining recently published molecular phylogenies (Bhattacharya & Price, 2020; Derelle et al., 2016; Li et al., 2020). Afterwards, we evaluated the phylogenetic signal in the area metric of cyanobacteria and microalgal groups applying the *phylosig* function available in the *phytools* R package (Revell, 2012). The calculated Pagel's λ varies from 0 to 1 and is considered as a measure of the degree of phylogenetic dependence in the data (Pagel, 1999).

2.6 | Size constraints of the shapes

To investigate how linear dimensions of the various morphologies limit their performance in the pelagic environment, we calculated Cs/Cv ratios for each selected taxon and these values were plotted against their largest possible linear dimensions found in the literature.

3 | RESULTS

The studied phylogenetic groups exhibited varying degrees of morphological diversity (Figure 2). Cyanobacteria covering a large area in the morphospace displayed the highest morphological variability. Single spheres, elongated filaments, star-like utricular and densely packed spherical coenobia are all present in this division. Among eukaryotic algae, Chrysophyceae, Chlorophyceae and Xanthophyceae were the morphologically most diverse lineages. These were followed by Trebouxiophyceae, Zygnematophyceae (Streptophyta) and Eustygmatophyceae, Synurophyceae, and Bacillariophyceae (all three groups belong to Stramenopiles), in which various forms of multicellular colonies occur. Among the unicellular flagellated groups, euglenoids and dinoflagellates showed the largest morphological diversity, due to the highly flattened and elongated shapes. Other unicellular groups having slightly elongated or drop-like cells were positioned along the borderline of the morphospace that connects the sphere to filaments.

The area metric of the algal groups showed the lack of phylogenetic dependence (Pagel's $\lambda = 0.4411$, $\log_{10}L = -28.1618$, $p = 0.9999$; Figure 3). Several sister groups (Xanthophyceae–Raphidophyceae; Zygnematophyceae–Klebsormidiophyceae; Chlorophyceae–Chlorodendrophyceae) showed remarkable differences in the size of occupied area (Figure 3).

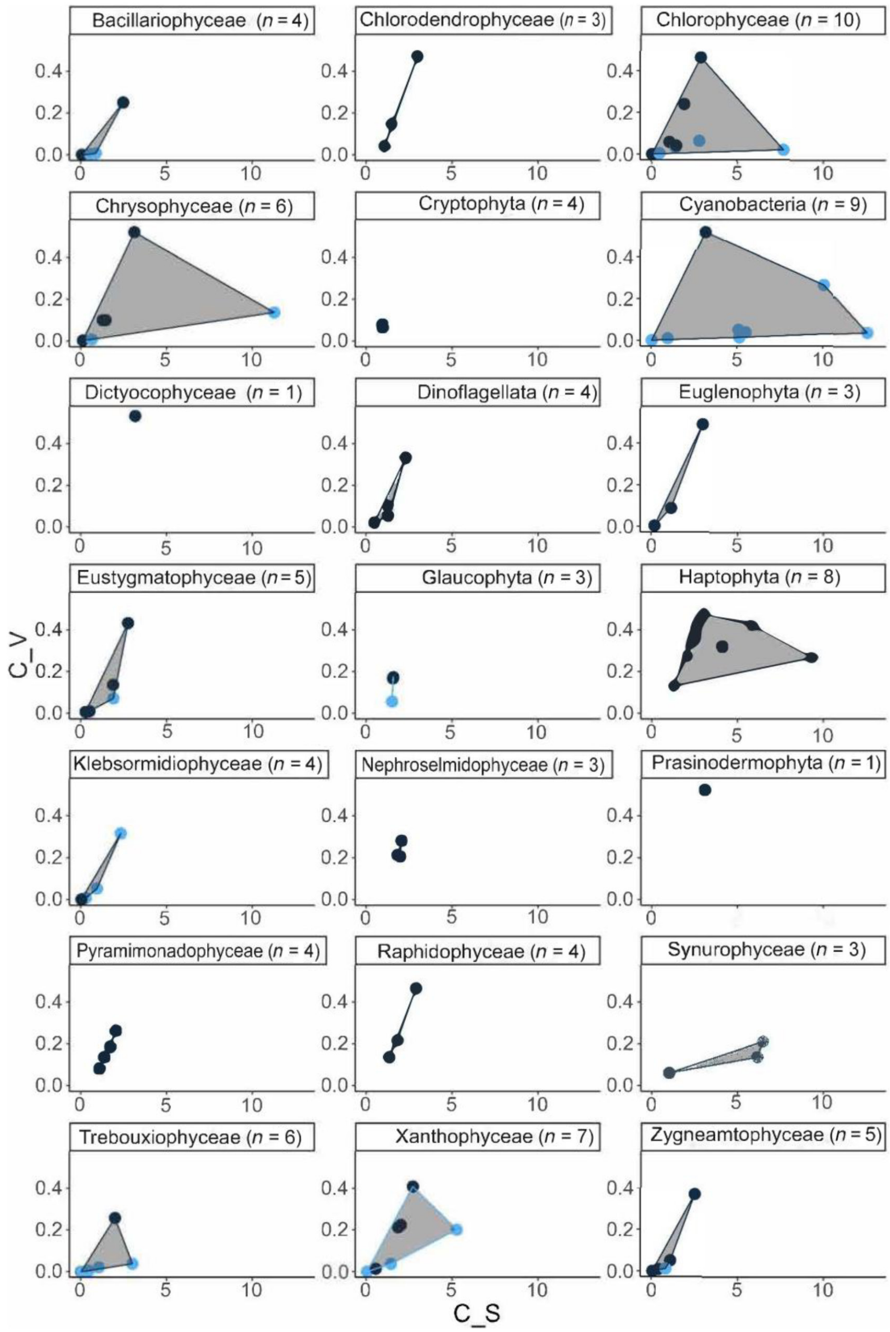

FIGURE 2 Areas occupied by cyanobacteria and the various algal groups in the *Cs*–*Cv* two-dimensional morphospace. Results are presented individually for each group. Black dots represent unicellular taxa, while blue triangles multicellular filaments and colonies

We found no relationship between the occupied area of the groups and their taxonomic diversity (Figure 4). Diatoms (Bacillariophyceae), which have large species diversity, covered only a medium-sized area in the morphospace.

Having the *Cs* and *Cv* values of the cyanobacteria and microalgae and their greatest axial linear dimensions (GALD) we positioned some representative objects in a *Cs*–*Cv*–*GALD* 3D place. The position of the cells and colonies indicated that *Cs* and *Cv* values of the objects set the range where values of GALD might potentially fall (Figure 5). To model what this graphical illustration suggests we plotted the GALD values of each 3D object against their *Cs/Cv* ratios (note that this is a non-dimensional shape attribute and is not identical to the surface area/volume ratio).

We observed a relationship between *Cs/Cv* ratios of the cyanobacteria and microalgae and their GALD values (Figure 6). The various shapes occupied different ranges of the size scale. Having the smallest *Cs/Cv* values, spherical or slightly ellipsoid forms were positioned at the lower size ranges. Linear dimensions of the non-flagellated representatives of this group could not exceed 30 µm. More complex forms ($C_S/Cv > 10$) were distributed in the middle and upper ranges of the size scale. These organisms constitute the micro- (20–200 µm) and mesoplankton (200–2000 µm) in the freshwater pelagial.

The length of single celled obligate autotrophic microalgae (●) with small (<10) *Cs/Cv* ratio did not exceed 25 µm (Figure 7). Above this length, single celled taxa were mixotrophic (○), or had

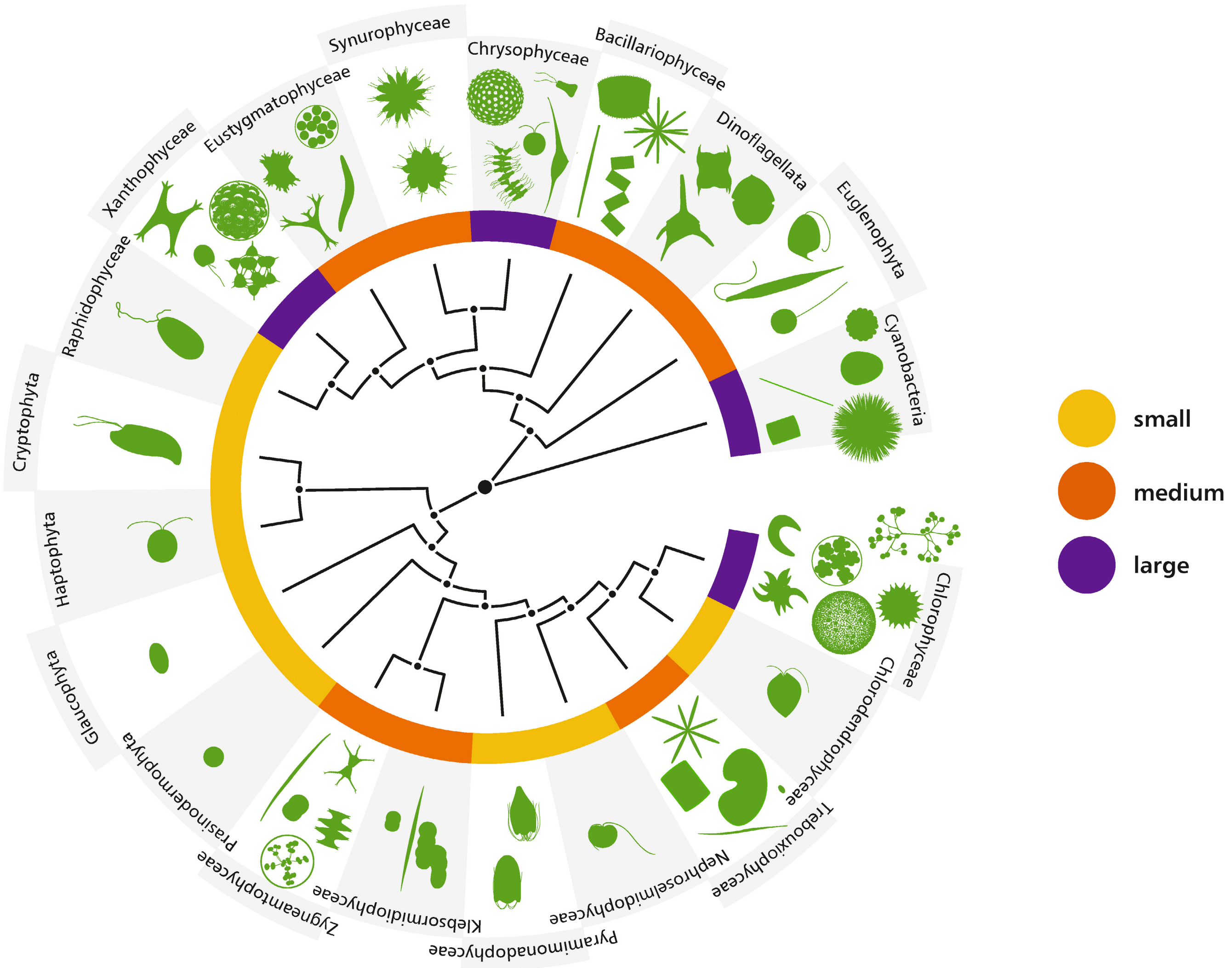

FIGURE 3 Phylogenetic tree of cyanobacteria and microalgae, based on recent results (Bhattacharya & Price, 2020; Derelle et al., 2016; Li et al., 2020). Colours indicate the area metrics of the groups applying log-scale intervals (yellow: 0–0.05, red: 0.05–0.5, purple: <0.5). Pictograms display the relevant algae considered in the analyses

considerably higher *Cs/Cv* ratios. Length of the colonial (multicellular) forms (x) exceeded 30 μm and their *Cs/Cv* ratios ranged above 10.

4 | DISCUSSION

To characterise the shape of particles, Wadell (1935) proposed the use of sphericity, defined as the ratio of the surface area of an equal-volume sphere to the actual surface area of the particle. Applying the inverse of this measure (the surface extension for unicellular marine phytoplankton) Ryabov et al. (2021) described relationships among cell morphology, size, and taxonomic diversity. While sphericity or surface extension are single numbers and represent a one-dimensional interpretation of morphology, here we proposed a 2D morphospace to reveal the morphological complexity and diversity of freshwater cyanobacteria and microalgae. The space has been defined by (i) surface shape factor (*Cs*), characterising the *coarseness* of the object surface, and a volumetric shape factor (*Cv*), characterising the shape deviation from a sphere. The first factor has small values for spindle-shaped, elongated ellipsoid and spherical shapes and increases when there are ridges or cavities on the surface of the object. The second factor increases when cell shape approaches the spherical shape and tends to zero for elongated shapes. Although *Cv* and *Cs* constants are basically used for calculating the volume and surface area of 3D objects, because of the above-mentioned characteristics they represent specific, biologically important aspects of the morphological complexity of cells and colonies.

We must note here that the present elaboration of the 3D models does not enable us to consider the fine structure of the cell surface (e.g. ornamentation of diatom frustules, skeletons of silicoflagellates), elaborate liths on a wide variety of coccolithophores, plates on dinoflagellates, which might affect the position of species in the morphospace. These details are outside of the scope of the present study.

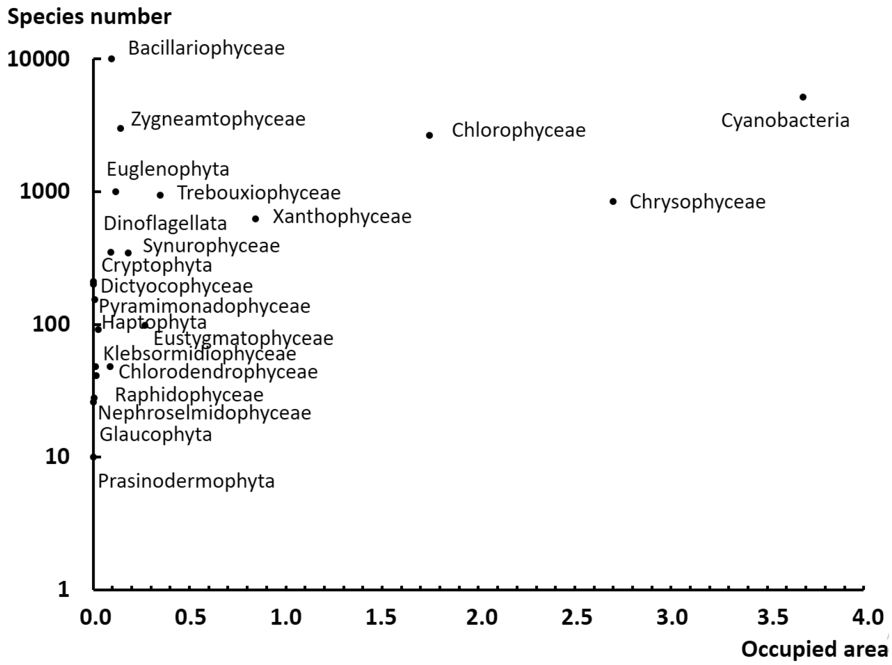

FIGURE 4 Distribution of the taxa in the occupied area–species number plot

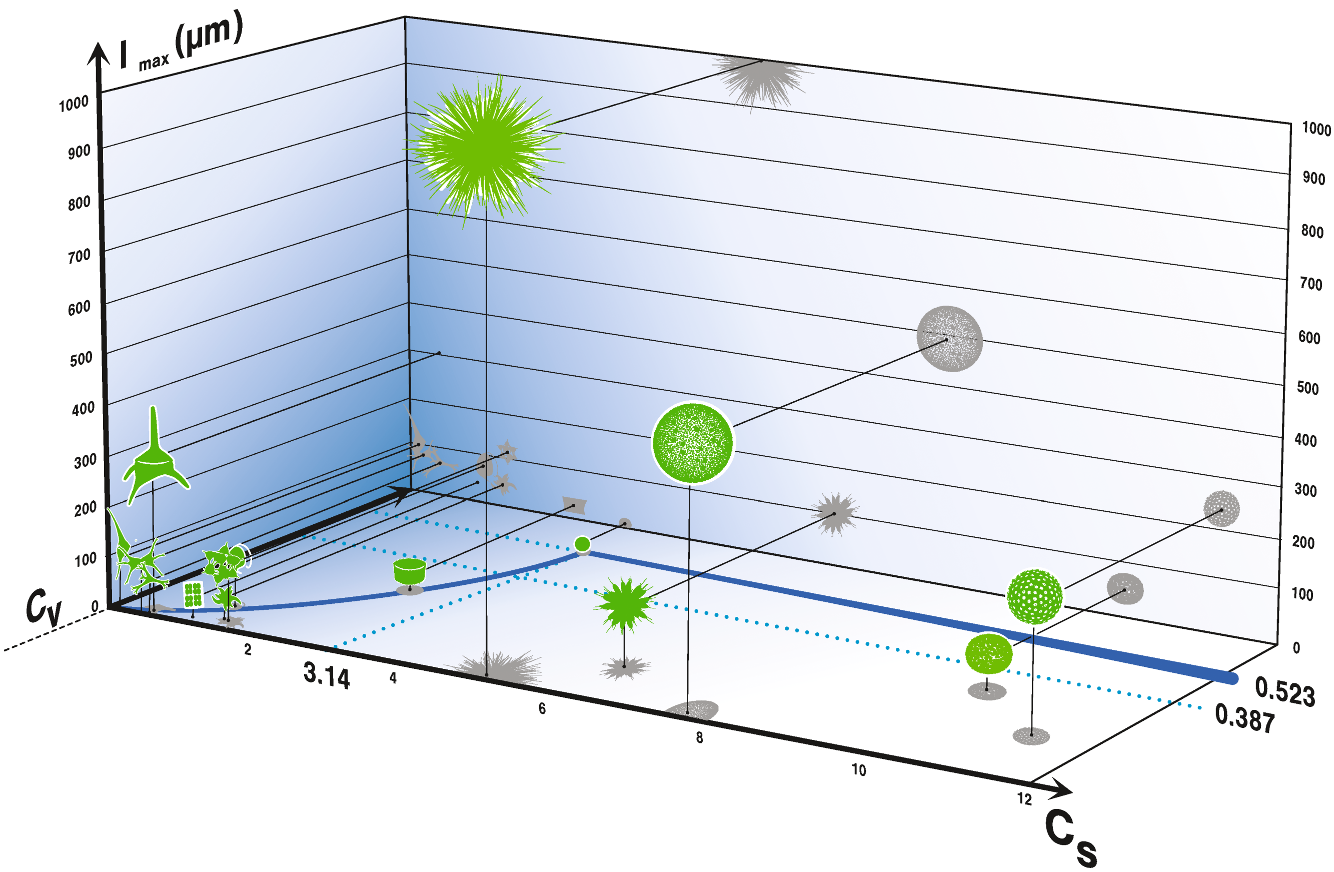

FIGURE 5 Position of selected algal taxa in a *Cs*-*Cv*-Imax (greatest axial linear dimensions) three-dimensional morphospace. The first two axes of the morphospace are the *Cs* and *Cv* constants, while the third is the maximum linear dimension of the objects, ranging from 0 to 1,000 μm

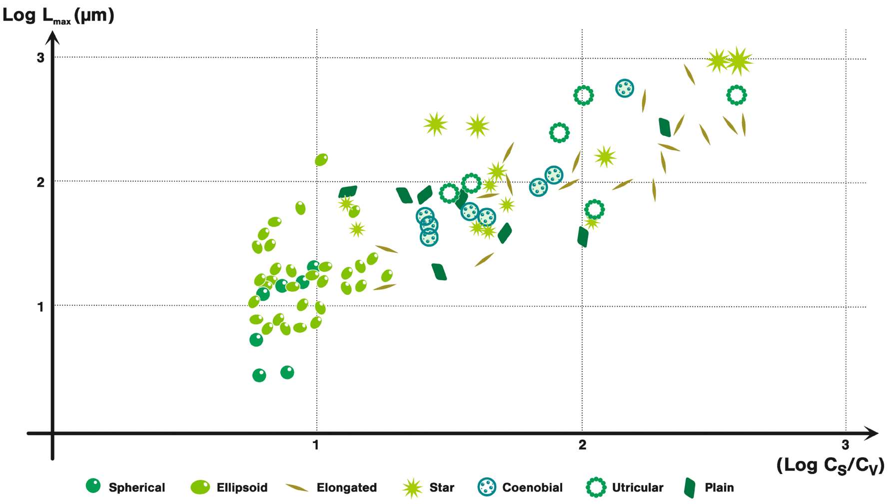

FIGURE 6 Relationship between the *Cs*/*Cv* ratios of taxa (X) and their largest linear dimensions (Y) at $\log_{10}$ scale. Each symbol represents a given taxon involved into the analysis. The colour and shape of the different symbols denote morphological categories

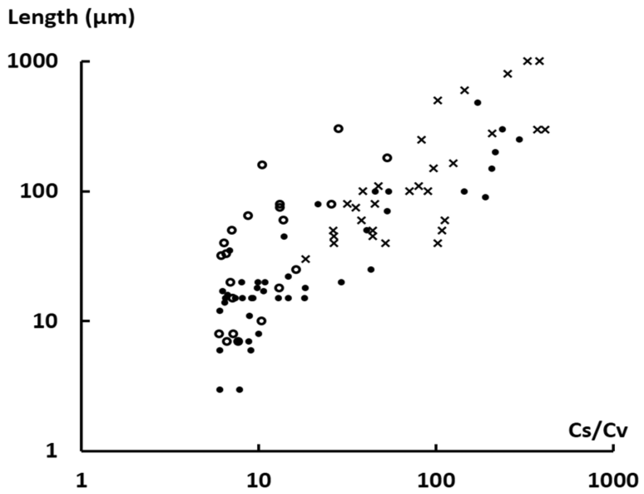

FIGURE 7 Distribution of single celled obligate autotrophic (●); single celled mixotrophic (○) and colonial (×) taxa in the *Cs*/*Cv*–length (greatest axial linear dimensions) plot

4.1 | Occupation of the morphospace by cyanobacteria and groups of microalgae

The various extant algal groups occupied different area sizes and different regions in the morphospace. The left part of the space appeared to be the most densely occupied region, where single-celled spheroids, oval, or drop-like and elongated forms were positioned along the borderline. These shapes dominate among unicellular algae in a marine environment (Ryabov et al., 2021). Single-celled groups covered small areas in the space, even in the case of those groups where cell-level morphological differences seemed to be large (Euglenophyceae, Zygnematophyceae). Only those groups attained high morphological diversity (i.e. covered large areas in the morphospace) that were capable of forming multicellular colonies with high *Cs* values.

Although the objects occupied clearly defined subspaces, the morphological evolution of algae found different ways of reaching the same goal, resulting in different shapes positioned in identical parts of the morphospace. Cyanobacteria outstandingly exemplify this pattern. Using spherical, oval, or barrel-shaped cells, cyanobacteria were able to develop each basic form: straight or coiled filaments, flat, star-shaped, utricular, loosely, or densely packed coenobia. Among these, star-shaped, utricular, and loosely packed coenobia can be identical in terms of their *Cs* and *Cv* values if they derive from the assembly of the same number of cells with identical shape, and the diameters of their colonies are also the same.

During the selection of morphologically different categories of the taxonomic groups, we aimed to find the extremities that define the maximum occupied area in the morphospace. However, this does not mean that the morphologies occupy only the edges of the allowed area. Since *Cs* values are strongly determined by the number of cells in colonies, they can vary greatly even at species level, and thus they can occupy the middle of the allowed area.

4.2 | Morphological diversity and evolutionary relatedness

The low value of Pagel's λ indicated that no phylogenetic signal is present, and thus morphology of cyanobacteria and microalgae evolved in response to selective processes independently of evolutionary relatedness. The large number of various shapes among cyanobacteria implies a link between morphological diversity and the evolutionary age of groups. However, it presumes that morphological differences among species accumulate continuously during evolution, which is rarely found in cladogenesis. The well-known mass extinction events affected not only the macroflora and fauna but also had serious consequences on the Earth's microbiota. These events coincided with the formation of novel habitats and extinction of competitors, and thus triggered speciation in formerly less successful lineages. Paleontological studies provide examples showing how a large diversity of related species may appear rapidly in the fossil record (Herron et al., 2009; Myers & Burbrink, 2012). The appearance of Stramenopiles in the Proterozoic and their radiation after the late Cretaceous mass extinction (Leyland et al., 2017; Yoon et al., 2009), the Streptophyte–Chlorophyte transition in the Permian–Triassic boundary, the morphological and genetic diversification of Chrysophyceae, Xanthophyceae, and Bacillariophyceae lineages in the Tertiary are well documented in fossil records (Martín-Closas, 2003).

The large differences experienced between morphological diversity of sister groups SUCH AS Xanthophyceae/Raphidophyceae or Chlorophyceae/Chlorodendrophyceae also demonstrate that the evolutionary age of the groups is not a good predictor of their morphological complexity. Prasinodermophyta (the third phylum of Viridiplantae), Pyramimonadophyceae (an early branching lineage of Chlorophyta), or Euglenophyceae also provide evidence for this statement. These lineages diverged in the Proterozoic and early Mesozoic without developing complex morphologies. The lack of otherwise geometrically possible forms in some lineages can be explained occasionally by the shortage of time, but most often, by developmental and functional constraints (McGhee, 2001). In the case of diatoms, the way cell division occurs and new valves of daughter cells are created, provides development constraints that do not enable the formation of utricular and densely packed spherical colonies. Despite the relatively low morphological diversity of diatoms, the number of species within this group is high, which suggests high physiological diversity (Brand, 1990). In the majority of groups, functional constraints presumably account for the empty regions in the morphospace, as the survival of newly emerging morphologies depends on how their fitness values relate to those of the already existing forms.

4.3 | Morphological convergences

The large overlaps between the areas covered by the various taxonomic groups indicates that similar forms can occupy remote branches of the tree of life. This result suggests a strong convergent evolution among distant lineages. The reason for the widespread morphological convergence among microalgae is that they live in a highly viscous media, under a low Reynolds number regime that governs the shape evolution of both motile and non-motile microorganisms (Reynolds, 2006). Flagellated motile organisms are perhaps the most obvious examples of this evolutionary process. Motion in highly viscous media requires the development of similar morphological adaptations. Although spherical, drop-like, or symmetrical fusiform shapes occur among these creatures, the asymmetric, slightly flattened helical forms are also frequent among flagellates. The reason for this is that a helical shape ensures approximately 15% contribution to propulsive thrust for flagellated directional swimmers (Constantino et al., 2016). Representatives of remote lineages such as Euglenophyta, Cryptophyta, Chlorophyceae, Chrysophyceae, or Raphydophyceae share these morphological features.

Cell-level morphological convergences can be observed even in the case of complex forms. Star-shaped unicells evolved in distant lineages of Streptophyta (*Staurastrum* spp.), Eustygmatophyceae (*Pseudostaurastrum* spp.), or Xanthophyceae (*Isthmochloron* spp.).

Shape convergences are much more common among multicellular organisms. The *proliferate and stick together* strategy resulted in various colony shapes, but these all can be traced back to the orientation of division planes and the way of sticking together after proliferation (Figure 8). These processes resulted in a finite number of colony forms, which repeatedly occurred during the evolution of distant cyanobacterial and microalgal lineages. With the formation of colonies, cyanobacteria and microalgae can increase their *Cs* and *Cv* values without considerable reduction in their surface area/volume ratio. The best examples are species with star-like colonies such AS *Ankistrodesmus* ssp. and *Gloeotrichia* spp., which can attain *c*. 10 times increase in their *Cs* and *Cv* values by increasing their cell (radius) numbers occasionally without any increase in their greatest axial linear dimensions and decrease in their surface area/volume ratios.

4.4 | Size constraints of single-celled and colonial forms

Because of their low surface area/volume ratios and high sinking velocity, the diameter of non-flagellated spherical or spheroid phytoplankters rarely exceeds 25–30 μm (*c*. $10^4 \mu m^3$) in freshwaters. This finding is consistent with that of a previous study (Mittler et al., 2019) in which the authors investigated the length–volume relations for phytoplankton communities and found that the shape distribution of planktic algae shifts to the dominance of elongated and complex forms with increasing length. Our results also show agreement with that of Ryabov et al. (2021), who studied unicellular elements of oceanic phytoplankton and found no tendency for elongation with increasing cell volume. Large (>25–30 μm) spherical algae in freshwaters are mixotrophic (i.e. they use dissolved and/or particulate organic sources to supplement their photoautotrophy) and they need to have flagellar apparatus to remain entrained in the water. Lacking these capabilities, the shape of large single-celled algae has to deviate markedly from sphere.

During microalgal evolution, deviations towards the spindle or needle shapes appeared in several lineages (Chlorophyceae, Klebsormidiophyceae, Zygnematophyceae, Bacillariophyceae). The elongated forms are considered as good adaptations to light deficient environments. Position of their photosynthetic pigments in the cells' periphery enables them to function as light antennae (Reynolds, 1998b). The other advantage of elongation is that elongated algae are more resistant to sinking, which gives them an advantage in low light conditions (Padisák et al., 2003).

The wide size range over which multicellular forms occur indicates that these forms successfully merged the ecological benefits of being small and large. During their evolution, cyanobacteria did not invest much into cell-level morphological differentiations. Instead, they became the champions in creating various morphologies using small building blocks (cells) and manipulating cell division planes. The

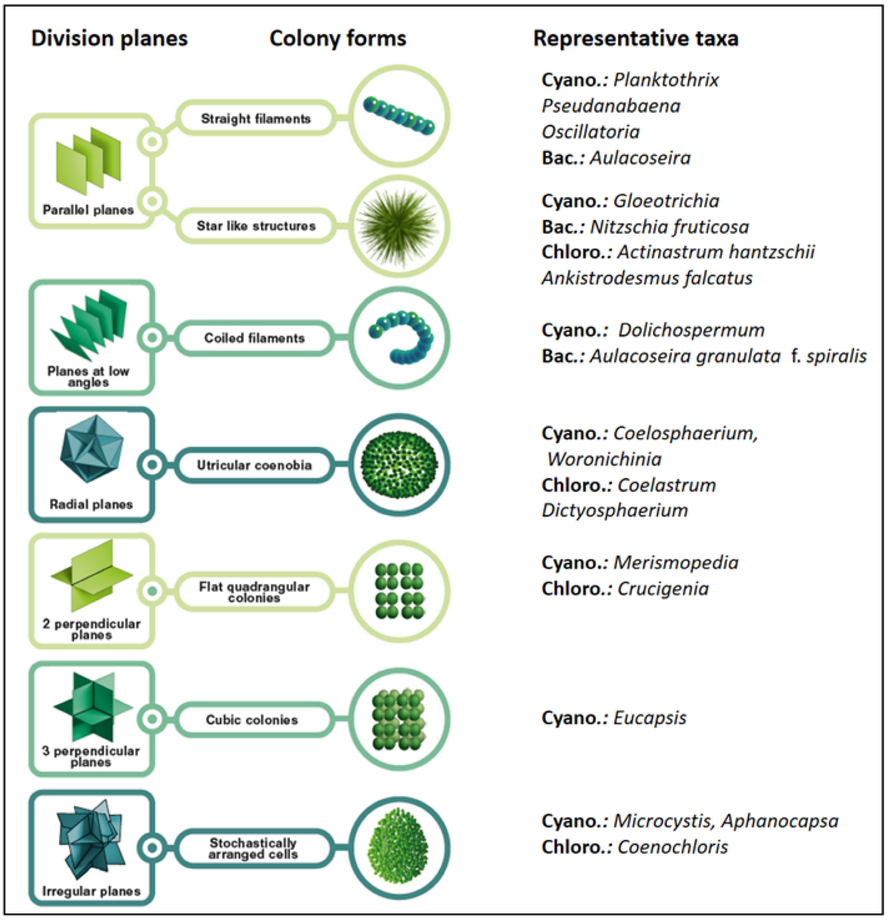

FIGURE 8 Orientation of division planes and the spatial organisation of the resulted colonies and some representative taxa. Cyano, Cyanobacteria; Bac, Bacillariophyceae; Chloro, Chlorophyta

size of the cells is usually constrained to 1–6 μm (<110 μm^3), which enables them to create variously shaped colonies at wide spatial dimensions (10–500 [1,000] μm) and to maintain high surface-to-volume ratios, even in large colonies.

Colony formation in other groups seems to be limited by cell size. Large-celled groups like euglenoids, dinoflagellates or raphydophytes do not form colonies. In large-celled colonies, the surface-to-volume ratios are larger than that of a single cell of similar diameter, but this increase incurs large fitness costs due to increased sinking velocity. This explains why the relatively large-celled, colonial planktic organisms (such as *Synura* spp.) are always motile and have alternative nutritional strategies (phagotrophy).

We found several forms positioned in the same region of the *Cs*/*Cv-GALD* space. These forms have similar surface area/volume ratios and greatest axial linear dimensions and can be considered as morphologically different but functionally similar adaptations to grazing, or to the various nutrient and light conditions.

5 | CONCLUSIONS

Using surface area (*Cs*) and volume constants (*Cv*) of 3D objects as axes, we defined a 2D Euclidean morphospace. We used this morphospace to: (1) describe the various morphologies occurring in microalgal and cyanobacterial lineages; (2) show how the various shapes relate to each other; (3) explain why multicellularity provide a selective advantage over unicellularity; and (4) characterise morphological complexity and diversity of the groups. We demonstrated that algal groups of freshwater phytoplankton show considerable differences in terms of their morphological diversity. We have shown that evolutionary relatedness is unrelated to morphological diversity, suggesting that the evolutionary age of taxa does not influence their morphologies.

Our results also suggest that the position of taxa in the *Cs*–*Cv* morphospace determines their largest attainable biovolume, because microalgae with low *Cs* values can attain large biovolumes if they have alternative nutritional strategies (mixotrophy, phagotrophy).

Because of the close linkage between phytoplankton morphology and ecology, the proposed morphospace may serve as a proxy for an ecospace. Thus, in the future, the proposed morphospace can be used to visualise current ecological processes such as eutrophication of waters or seasonal succession of phytoplankton.

AUTHOR CONTRIBUTIONS

Conceptualisation: G.B., V.L., Z.V.; conducting the research and data analysis: J.F., G.V., Z.V.; developing methods: G.B., J.F.; preparation of figures and tables: G.V., V.L., Z.V.; data interpretation: G.B., Z.V., E.T.K., J.G., V.B.-B., V.L. All authors read and approved the final manuscript.

ACKNOWLEDGMENTS

This work was supported by Hungarian Scientific Research Fund (NKFIH OTKA) project no.: K-132150. On behalf of Project TetraClim, we thank for the usage of ELKH Cloud (https://science-cloud.hu/) that significantly contributed to perform the phylogenetic analyses.

DATA AVAILABILITY STATEMENT

The analysed data are available at the repository "Concordia": https://science-data.hu/dataset.xhtml?persistentId=hdl:21.15109/CONCORDA/FNSHPU.

ORCID

Gábor Várbíró https://orcid.org/0000-0001-5907-3472

REFERENCES

Bhattacharya, D., & Price, D. C. (2020). The algal tree of life from a genomics perspective. In A. Larkum, A. Grossman, & J. Raven (Eds.), *Photosynthesis in algae: Biochemical and physiological mechanisms. Advances in photosynthesis and respiration* (Vol. *45*, pp. 11–24). Springer.

Blender Foundation and Community. (2020). *"Blender." (Version 2.91) Amsterdam*. Stichting Blender Community. http://www.blender.org/download/

Borics, G., Lerf, V., Enikő, T., Stanković, I., Pickó, L., Béres, V., & Várbíró, G. (2021). Biovolume and surface area calculations for microalgae, using realistic 3D models. *The Science of the Total Environment*, *773*, 145538.

Brand, L. E. (1990). Review of genetic variation in marine phytoplankton species and the ecological implications. *Biological Oceanography*, *6*, 397–409.

Carroll, S. B. (2001). Chance and necessity: The evolution of morphological complexity and diversity. *Nature*, *409*(6823), 1102–1109.

Constantino, M. A., Jabbarzadeh, M., Fu, H. C., & Bansil, R. (2016). Helical and rod-shaped bacteria swim in helical trajectories with little additional propulsion from helical shape. *Science Advances*, *2*(11), e1601661.

Derelle, R., López-García, P., Timpano, H., & Moreira, D. (2016). A phylogenomic framework to study the diversity and evolution of stramenopiles (= heterokonts). *Molecular Biology and Evolution*, *33*(11), 2890–2898.

Durante, G., Basset, A., Stanca, E., & Roselli, L. (2019). Allometric scaling and morphological variation in sinking rate of phytoplankton. *Journal of Phycology*, *55*(6), 1386–1393.

Falkowski, P.G., Katz, M. E., Knoll, A. H., Quigg, R., Raven, J. A., Schofield, O., & Taylor, F. J. R., (2004). The evolution of modern eukaryotic phytoplankton. *Science*, *305*(5682), 354–360.

Gallet, R., Violle, C., Fromin, N., Jabbour-Zahab, R., Enquist, B. J., & Lenormand, T. (2017). The evolution of bacterial cell size: the internal diffusion-constraint hypothesis. *The ISME Journal*, *11*, 1559–1568.

Gerloff-Elias, A., Barua, D., Mölich, A., & Spijkerman, E. (2006). Temperature-and pH-dependent accumulation of heat-shock proteins in the acidophilic green alga *Chlamydomonas acidophila*. *FEMS Microbial Ecology*, *56*(3), 345–354.

Grover, J. P. (1989). Influence of cell shape and size on algal competitive ability. *Journal of Phycology*, *25*(2), 402–405.

Guiry, M. D. &, Guiry, G. (2008). *AlgaeBase*. AlgaeBase.

Herron, M. D., Hackett, J. D., Aylward, F. O., & Michod, R. E. (2009). Triassic origin and early radiation of multicellular volvocine algae. *Proceedings of the National Academy of the United States of America*, *106*(9), 3254–3258.

Hillebrand, H., Dürselen, C. D., Kirschtel, D., Pollingher, U., & Zohary, T. (1999). Biovolume calculation for pelagic and benthic microalgae. *Journal of Phycology*, *35*(2), 403–424.

Hoek, C., Mann, D., Jahns, H. M., & Jahns, M. (1995). *Algae: An introduction to phycology*. Cambridge University Press.

Jorstad, A., Nigro, B., Cali, C., Wawrzyniak, M., Fua, P., & Knott, G. (2015). NeuroMorph: A toolset for the morphometric analysis and visualization of 3D models derived from electron microscopy image stacks. *Neuroinformatics*, *13*(1), 83–92.

Karp-Boss, L., & Boss, E. (2016). The elongated, the squat and the spherical: Selective pressures for phytoplankton shape. In P. Glibert & T. Kana (Eds.), *Aquatic microbial ecology and biogeochemistry: A dual perspective* (pp. 25–34). Springer.

Kepler, J. (1611). *Strena seu de nive sexangula*. Godefrid Tampach.

Koch, A. L., Higgins, M. L., & Doyle, R. J. (1982). The role of surface stress in the morphology of microbes. *Journal of General Microbiology*, *128*(5), 927–945.

Leyland, B., Leu, S., & Boussiba, S. (2017). Are thraustochytrids algae? *Fungal Biology*, *121*(10), 835–840.

Li, L., Wang, S., Wang, H., Sahu, S. K., Marin, B., Li, H., ... Reder, T. (2020). The genome of *Prasinoderma coloniale* unveils the existence of a third phylum within green plants. *Nature Ecology and Evolution*, *4*(9), 1220–1231.

Litchman, E., & Klausmeier, C. A. (2008). Trait-based community ecology of phytoplankton. *Annual Review of Ecology, Evolution, and Systematics*, *39*, 615–639.

Litchman, E., Klausmeier, C. A., Schofield, O. M., & Falkowski, P. G. (2007). The role of functional traits and trade-offs in structuring phytoplankton communities: scaling from cellular to ecosystem level. *Ecology Letters*, *10*, 1170–1181.

Martín-Closas, C. (2003). The fossil record and evolution of freshwater plants: A review. *Geologica Acta*, *1*(4), 315–338.

McGhee, G. R. (2001). Exploring the spectrum of existent, nonexistent and impossible biological form. *Trends in Ecology and Evolution*, *16*(4), 172–173.

Mitsui, A., Kumazawa, S., Takahashi, A., Ikemoto, H., Cao, S., & Arai, T. (1986). Strategy by which nitrogen-fixing unicellular cyanobacteria grow photoautotrophically. *Nature*, *323*(6090), 720–722.

Mittler, U., Blasius, B., Gaedke, U., & Ryabov, A. B. (2019). Length–volume relationship of lake phytoplankton. *Limnology and Oceanography: Methods*, *17*(1), 58–68.

Myers, E. A., & Burbrink, F. T. (2012). Ecological opportunity: Trigger of adaptive radiation. *Nature Education Knowledge*, *3*(10), 23.

Naselli-Flores, L., & Barone, R. (2011). Invited review-fight on plankton! Or, phytoplankton shape and size as adaptive tools to get ahead in the struggle for life. *Cryptogamie, Algologie*, *32*(2), 157–204.

Naselli-Flores, L., Zohary, T., & Padisák, J. (2021). Life in suspension and its impact on phytoplankton morphology: An homage to Colin S. Reynolds. *Hydrobiologia*, *848*(1), 7–30.

Padisák, J., & Naselli-Flores, L. (2021). Phytoplankton in extreme environments: importance and consequences of habitat permanency. *Hydrobiologia*, *848*(1), 157–176.

Padisák, J., Soróczki-Pintér, É., & Rezner, Z. (2003). Sinking properties of some phytoplankton shapes and the relation of form resistance to morphological diversity of plankton—an experimental study. *Hydrobiologia*, *500*, 243–257.

Pagel, M. (1999). Inferring the historical patterns of biological evolution. *Nature*, *401*, 877–884.

Pasciak, W. J., & Gavis, J. (1974). Transport limitation of nutrient uptake in phytoplankton. *Limnology and Oceanography*, *19*, 881–888.

Planavsky, N. J., Asael, D., Hofmann, A., Reinhard, C. T., Lalonde, S. V., Knudsen, A., ... Beukes, N. J. (2014). Evidence for oxygenic photosynthesis half a billion years before the Great Oxidation Event. *Nature Geoscience*, *7*(4), 283–286.

R Core Team. (2018). *R: A language and environment for statistical computing*. R Foundation for Statistical Computing.
Raven, J. A. (2010). Inorganic carbon acquisition by eukaryotic algae: Four current questions. *Photosynthesis Research*, *106*(1), 123–134.
Revell, L. J. (2012). phytools: An R package for phylogenetic comparative biology (and other things). *Methods in Ecology and Evolution*, *3*, 217–223. https://doi.org/10.1111/j.2041-210X.2011.00169.x
Reynolds, C. S. (1998a). Plants in motion: Physical–biological interactions in the plankton. In J. Imberger (Ed.), *Physical processes in lakes and oceans*. *Coastal and estuarine studies 54* (pp. 535–560). American Geophysical Union.
Reynolds, C. S. (1998b). What factors influence the species composition of phytoplankton in lakes of different trophic status? *Hydrobiologia*, *369/370*, 11–26.
Reynolds, C. S. (2006). *The ecology of phytoplankton*. Cambridge University Press.
Rimet, F., & Bouchez, A. (2012). Life-forms, cell sizes and ecological guilds of diatoms in European rivers. *Knowledge and Management of Aquatic Ecosystems*, *406*, 1283–1299.
Ryabov, A., Kerimoglu, O., Litchman, E., Olenina, I., Roselli, L., Basset, A., … Blasius, B. (2021). Shape matters: the relationship between cell geometry and diversity in phytoplankton. *Ecology Letters*, *24*(4), 847–861.
Sloane, N. J. (1998). Kepler's conjecture confirmed. *Nature*, *395*(6701), 435–443.
Sournia, A. (1982). Form and function in marine phytoplankton. *Biological Reviews*, *57*(3), 347–394.
Stoddard, M. C., Yong, E. H., Akkaynak, D., Sheard, C., Tobias, J. A., & Mahadevan, L. (2017). Avian egg shape: Form, function, and evolution. *Science*, *356*(6344), 1249–1254.
Sukumar, S. R., Page, D. L., Koschan, A. F., & Abidi, M. A. (2008). June. Towards understanding what makes 3D objects appear simple or complex. In *2008 IEEE Computer Society Conference on Computer Vision and Pattern Recognition Workshops* (pp. 1–8). IEEE.
Sun, J., & Liu, D. (2003). Geometric models for calculating cell biovolume and surface area for phytoplankton. *Journal of Plankton Research*, *25*(11), 1331–1346.
T-Krasznai, E., Lerf, V., Tóth, I., Kisantal, T., Várbíró, G., Vasas, G., … Borics, G. (2022). Uncertainties of cell number estimation in cyanobacterial colonies and the potential use of sphere packing. *Harmful Algae*, *117*, 102290.
Wadell, H. (1935). Volume, shape, and roundness of quartz particles. *The Journal of Geology*, *43*(3), 250–280.
Watanabe, A., Fabre, A. C., Felice, R. N., Maisano, J. A., Müller, J., Herrel, A., & Goswami, A. (2019). Ecomorphological diversification in squamates from conserved pattern of cranial integration. *Proceedings of the National Academy of the United States of America*, *116*(29), 14688–14697.
Yoon, H. S., Andersen, R. A., Boo, S. M., & Bhattacharya, D. (2009). Stramenopiles. In M. Schaechter (Eds.), *Encyclopedia of microbiology* (pp. 721–731). Elsevier Inc.

SUPPORTING INFORMATION

Additional supporting information can be found online in the Supporting Information section at the end of this article.

How to cite this article: Borics, G., Várbíró, G., Falucskai, J., Végvári, Z., T-Krasznai, E., Görgényi, J., B-Béres, V., & Lerf, V. (2023). A two-dimensional morphospace for cyanobacteria and microalgae: Morphological diversity, evolutionary relatedness, and size constraints. *Freshwater Biology*, *68*, 115–126. https://doi.org/10.1111/fwb.14013